Modulational instability with higher-order dispersion and walk-off in Kerr media with cross-phase modulation

K. Nithyanandan,[1] R. Vasantha Jayakantha Raja,[2] K. Porsezian,[1] and B. Kalithasan[3]
[1]*Department of Physics, Pondicherry University, Pondicherry 605014, India*
[2]*Department of Physics, Central University of Tamil Nadu, Thiruvarur 610004, India*
[3]*Department of Physics, Chennai Institute of Technology, Nandhambakam, Chennai 600069, India*
(Received 12 April 2012; published 17 August 2012)

We investigate the cross-phase-modulation-induced modulational instability (MI) of two co-propagating optical beams in the system of relaxing Kerr nonlinearity with the effect of higher-order dispersion (HOD) and walk-off effect. We identify and discuss the salient features of relaxation of nonlinear responses and HOD using suitable theoretical model. First, we analyzed the impact of HOD and walk-off on the MI spectrum and found both analytically and numerically that the MI exhibits alternate characteristics like the evolution of different spectral bands in addition to the conventional MI bands. The walk-off effects in the virtue of HOD not only consist of the conventional group velocity mismatch (GVM) but also the difference in third-order dispersion (TOD) of the two beams, and thereby significantly modify the dynamical behavior of the MI. We also consider the combined effect of relaxation of nonlinear response and the HOD effects, and we observe that any finite value of delay leads to the evolution of two unstable modes and thereby extends the range of unstable frequency; HOD on the other hand along with the walk-off effect brings other characteristic spectral bands. A detailed discussion about the various combinations of parameters and the relative competence of one over the other on the MI spectrum is presented. Thus the evolution of MI from cross-phase modulation in the system of relaxing Kerr nonlinearity is emphasized in detail and the influence of HOD and the walk-off effect are highlighted.

DOI: 10.1103/PhysRevA.86.023827 PACS number(s): 42.65.Tg, 42.65.Wi, 42.81.Dp

I. INTRODUCTION

Co-propagation of two intense optical beams in a dielectric media may lead to a pool of information about the various physical effects in the world of nonlinear physics [1–7]. The coupling of these two beams result in many fascinating effects like modulational instability (MI), four-wave mixing (FWM), stimulated Raman scattering (SRS), and so on. One such phenomenon is the MI, which is considered to be a central process in nonlinear optics. MI is an instability process, whereby a continuous wave (CW) or quasi-CW undergoes an exponential growth of the weak perturbation under the conservative interaction between nonlinear and dispersive effects. The perturbation can originate either from quantum noise or from the frequency shifted signal; accordingly MI can be called spontaneous MI or induced MI [1]. In the context of optical fiber, the generation of ultrashort solitonlike pulse trains using MI was proposed theoretically by Hasegawa in 1984 [8]. Later, the experimental realization was given by Tai *et al*. [9] in 1986. After this seminal work, MI has attracted a lot of attention and evolves as the subject of intense investigation due to numerous potential applications in various diverse fields.

MI until now has been addressed in two distinct directions based on its fundamental and applied interest. The two distinct perceptions are exactly in the opposite sense, where one deals with the catastrophic effects and the other presents the exuberance of its usefulness in the various applications. The deleterious effects of MI are detrimental to the long-haul optical fiber communication system: The non-return-to-zero code in optical communication, the drastic enhancement of MI gain in the WDM system sets the limitation to the bandwidth window of the communication system, MI lasers, and new frequency generation in optical systems are the ultimate concern for the realization of a repeater-less long-haul optical communication system [10,11]. Quite a good number of works have been devoted to address the above highlighted issues with the objective of reducing the disastrous effects caused by MI. Equally, another side of the literature, especially the contemporary research activities, focused primarily on the constructive part of the MI. For example, generation of pulse trains at a high repetition rate is a useful technique to produce the ultrashort pulses; frequency conversion and the generation of new frequencies can be effectively made useful in the multifrequency source under the context of supercontinuum generation, which has been recognized in modern days as "white-light laser" [12–14]. In addition, MI has also found important applications in optical amplification of weak signal, material absorption and loss compensation [15,16], dispersion management, all-optical switching [17], frequency comb for metrology, and so on [18–20]. Thus a suitable manipulation with a clinical tailoring can make MI a suitable contender for a wide class of applications. Our strategic view in the present work is rather focused on the constructive side, precisely in the new frequency generation by enhancing and appreciating the MI effects in the fiber.

In the context of optical fibers, the MI analysis is deeply connected with the nonlinear Schrödinger equation (NLSE) which leads to the formation of soliton or solitary wave by virtue of the delicate balance between anomalous group velocity dispersion (GVD) and self-phase modulation (SPM) [1,7,21]. Depending on the power of the intense beam, by incorporating the various physical effects, the NLSE can be extended and the different physical phenomena can be studied. In recent times, much attention has been paved towards the understanding of the role of relaxation of nonlinear response on the MI [22–28]. It is worth noting that the usual assumption of instantaneous Kerr response fails for ultrashort pulses,

thereby the inclusion of delay in the nonlinear response is very much essential. In the context of spatial MI, due to the noninstantaneous nature of the nonlinear response MI is observed both in self-focusing and self-defocusing medium [23]. Spatiotemporal MI with finite response time has been observed in Refs. [24,25]. The role of the Raman delayed response on the MI sideband has been explained in Ref. [29]. Recently, Liu *et al*. analyzed exclusively the impact of finite relaxation time in the MI spectrum by considering a simple model called the Debye relaxational model [22]. The authors have predicted that the role of delay is crucial in determining the gain of the MI and also found the inclusion of any finite relaxation time extends the range of unstable frequencies [22]. In Ref. [30], the authors have followed such a relaxational model as in Ref. [22], and analyzed the combined effect of relaxation and saturation of nonlinearity in the MI spectrum. They have reported the existence of two unstable bands in the anomalous GVD regime, namely, instantaneous and Raman band. MI is observed even in the normal GVD regime with the aid of the finite relaxation time, but instead of two unstable bands, only a single band is observed [30].

All the above cases considered the propagation of a single optical beam down the fiber; MI of such a kind is termed the scalar MI. The co-propagation of two or more optical beams inside the fiber can lead to interesting and peculiar phenomena which could not be realized in the single beam case. As a matter of fact, one of the breakthroughs in the field of nonlinear optics is the observation of MI in the normal GVD by Agrawal *et al*. [4–6]. It is a well proven fact that the propagation of the optical beam in the normal GVD regime is not subject to the MI process, due to the lack of phase matching between the dispersion and nonlinear components of the system. But the nonlinear coupling between the two co-propagating beams due to the cross-phase modulation (XPM) (i.e., refractive index seen by one wave depends on the intensity of the co-propagating wave through the XPM coefficient) destabilize the steady state leading to frequency modulation even in the normal GVD regime [31–33]. This pioneering work of Agrawal *et al*. set the benchmark for the extensive work on two-color light propagation in the optical fiber system. Thereafter numerous theoretical and experimental works were reported based on the wave propagation dynamics in birefringent fibers and also on the dual frequency pumping in the standard single-mode fiber.

For instance, a comprehensive idea of the ultrashort pulse generation in the normal dispersion regime of a birefringent fiber using MI was discussed in Refs. [34–39]. The existence of a nonlinear gap and the critical regime of MI was illustrated in Refs. [40,41]. A complete interplay between MI and SRS and the relative dominance of one over the other like the suppression of SRS and the enhancement of MI for the ultrashort pulse generation can be seen from Refs. [42–45]. Our intensive literature survey suggests that there has been only limited work available in the context of relaxing the nonlinear medium concerning the coupled system. In Ref. [28] MI is investigated in the noninstantaneous nonlinear media under two-beam propagation following the report of Refs. [17,46]. Recently, Canabarro *et al*. [47] have considered the combined effect of relaxing nonlinearity and the XPM-induced MI in the normal GVD regime.

What concerns the effect of HOD is as follows: When the width of the optical pulse is short enough, or when the light propagation is near the so-called zero dispersion wavelength (ZDW), the HOD will inevitably take effect [48,49]. Cavalcanti *et al*. [49] analyzed the MI near the ZDW and predicted the possibility of MI even at the normal GVD regime provided the fourth-order dispersion takes negative values, thereby serving for the necessary phase-matching condition. Pitois *et al*. [50] have experimentally observed the generation of a new spectral window by fourth-order dispersion. Dinda *et al*. [45,51], with their detailed analytical and numerical analysis, explained the various interesting behavior of MI under the combined effect of HOD and delayed Raman response. A concise analysis of the MI and SRS in the normally dispersive birefringent fiber can be seen in Ref. [52]. Moreover, inclusion of HOD also qualitatively changes the walk-off effect between the co-propagating beams thereby significantly modifying the MI spectrum. The emergence of a new spectral band due to the interplay between HOD and walk-off on XPM was discussed in Ref. [53]. Although the combined effect of the relaxing nonlinearity and XPM in normal GVD regime has been discussed in Ref. [47], however, it is limited only to the case of second-order dispersion. There has been no report to the best of our knowledge that brings the cumulative effect of relaxation of nonlinearity, HOD, and walk-off effect in the XPM-induced MI spectrum. Thus, considering the importance of HOD and walk-off effect in the MI dynamics, we in this article intent to investigate the interplay between the HOD and walk-off effect in the XPM-induced MI spectrum in the system of relaxing nonlinear response.

The paper is organized as follows: Following the detailed introduction in Sec. I, Sec. II features the theoretical model of the underlined problem, followed by the MI analysis in Sec. III. The paper is twofold: In Secs. IV and V, the influence of HOD and walk-effect in the MI spectrum are discussed in normal and anomalous dispersion regime, respectively. Later, Secs. VI and VII include the delay in the nonlinear response and bring the exclusive investigation of the interplay between various physical effects in the MI spectrum for both the dispersion regimes. Section VIII features the detailed summary and conclusion.

II. THEORETICAL MODEL

The co-propagation of two optical waves of different frequencies and the same polarization in the single-mode optical fiber is given by the coupled nonlinear Schrödinger equation (CNLSE). The general form of the CNLSE for the slowly varying envelope $E_j(z,t)$ corresponding to the co-propagation of optical beams along z axis with a group velocity V_{gj} in a retarded time frame $t = (T - z/V_g)$ is given by Refs. [4,47,52]

$$\frac{\partial E_j}{\partial z} + \frac{1}{V_{gj}}\frac{\partial E_j}{\partial t} + i\frac{\beta_{2j}}{2}\frac{\partial^2 E_j}{\partial t^2} - \frac{\beta_{3j}}{6}\frac{\partial^3 E_j}{\partial t^3} + i\frac{\beta_{4j}}{24}\frac{\partial^4 E_j}{\partial t^4} = i\gamma_j(|E_j|^2 + 2|E_{3-j}|^2)E_j, \quad (1)$$

where z and t are the longitudinal coordinate and time in the moving reference frame, respectively. V_{gj} $(j = 1,2)$ is the

group velocity. The dispersion coefficient β_{kj} ($k = 1,2,3,4$) attributes the Taylor expansion of the propagation constant around the center frequency ω_0. It is a proven fact that HOD plays a crucial role in the MI dynamics. Among HOD, fourth-order dispersion (FOD) plays a significant role in many of the practicable operating conditions. HODs beyond FOD are immaterial due to their small magnitude, unless and until included with any physical meaning to the desired problem, thus we limit our analysis only up to FOD, where $\gamma = \frac{n_2\omega_0}{cA_{\text{eff}}}$ is the Kerr parameter, n_2 is the nonlinear index coefficient, and A_{eff} is the effective core area.

In order to account for the delay in the nonlinear response, a simple relaxational model termed the Debye relaxational model is considered as in Ref. [22]. The dynamical equation governing the evolution of the envelopes of the co-propagating field can be written as a set of coupled equations as follows:

$$\frac{\partial E_j}{\partial z} + \frac{1}{V_{gj}}\frac{\partial E_j}{\partial t} + i\frac{\beta_{2j}}{2}\frac{\partial^2 E_j}{\partial t^2} - \frac{\beta_{3j}}{6}\frac{\partial^3 E_j}{\partial t^3} + i\frac{\beta_{4j}}{24}\frac{\partial^4 E_j}{\partial t^4} = i\gamma_j N_j E_j, \tag{2a}$$

$$\tau\frac{\partial N_j}{\partial t} = (-N_j + |E_j|^2 + 2|E_{3-j}|^2), \tag{2b}$$

where $N_j = N_j(z,t)$ is the nonlinear index of the medium and τ represents the finite response time of the medium.

III. MODULATIONAL INSTABILITY ANALYSIS

A. Linear stability analysis

The stability of the steady-state solution against small perturbation for the above dynamical equation is studied using linear stability analysis. In the continuous wave limit, the steady-state solution can be written as

$$E_j^{\text{CW}} = E_j^0 \exp\left[i\gamma_j\left(\left|E_j^0\right|^2 + 2\left|E_{3-j}^0\right|^2\right)z\right], \tag{3a}$$

$$N_j^{\text{CW}} = \left|E_j^0\right|^2 + 2\left|E_{3-j}^0\right|^2. \tag{3b}$$

To analyze the stability of the steady state against small perturbation, we perturb the steady state with a perturbed field of the following form:

$$E_j = \left[E_j^0 + a_j(z,t)\right]\exp\left[i\gamma_j\left(\left|E_j^0\right|^2 + 2\left|E_{3-j}^0\right|^2\right)z\right], \tag{4a}$$

$$N_j = n_j(z,t) + \left(\left|E_j^0\right|^2 + 2\left|E_{3-j}^0\right|^2\right), \tag{4b}$$

where $a_j(z,t)$ is the small perturbation satisfying $|a_j(z,t)|^2 \ll |E_j^0|^2$ and $n_j(z,t)$ is the small deviation from the stationary solution of the nonlinear index. Using Eq. (4) in Eq. (2), we obtain the linearized equation for the perturbations $a_j(z,t)$ and $n_j(z,t)$ as follows:

$$\frac{\partial a_j}{\partial z} + \frac{1}{V_{gj}}\frac{\partial a_j}{\partial t} + i\frac{\beta_{2j}}{2}\frac{\partial^2 a_j}{\partial t^2} - \frac{\beta_{3j}}{6}\frac{\partial^3 a_j}{\partial t^3} + i\frac{\beta_{4j}}{24}\frac{\partial^4 a_j}{\partial t^4} = i\gamma_j n_j E_j^0, \tag{5a}$$

$$\tau\frac{\partial n_j}{\partial t} = -n_j + E_j^0(a_j + a_j^*) + 2E_{3-j}^0(a_{3-j} + a_{3-j}^*). \tag{5b}$$

We assume the following ansatz for the perturbations with frequency detuning from the pump Ω, and k will be the wave number of the perturbation.

$$a_j(z,t) = U_j\exp[-i(kz - \Omega t)] + V_j\exp[i(kz - \Omega t)], \tag{6a}$$

$$n_j(z,t) = U_j\exp[-i(kz - \Omega t)] + V_j\exp[i(kz - \Omega t)], \tag{6b}$$

where U and V are the perturbation amplitudes corresponding to the anti-Stokes and Stokes sidebands, respectively. Solving the above linearized equation one will arrive at a set of four homogenous equations for U_j and V_j. Collecting the linear terms in U_j and V_j, one will arrive at the 4×4 stability matrix as follows:

$$D(\Omega) \equiv \beta_{21}\frac{\Omega^2}{2} - \beta_{31}\frac{\Omega^3}{6} + \beta_{41}\frac{\Omega^4}{24}, \tag{7a}$$

$$\tilde{D}(\Omega) \equiv \beta_{21}\frac{\Omega^2}{2} + \beta_{31}\frac{\Omega^3}{6} + \beta_{41}\frac{\Omega^4}{24}, \tag{7b}$$

$$E(\Omega) \equiv \beta_{22}\frac{\Omega^2}{2} - \beta_{32}\frac{\Omega^3}{6} + \beta_{42}\frac{\Omega^4}{24}, \tag{7c}$$

$$\tilde{E}(\Omega) \equiv \beta_{22}\frac{\Omega^2}{2} + \beta_{32}\frac{\Omega^3}{6} + \beta_{42}\frac{\Omega^4}{24}, \tag{7d}$$

$$\tilde{\gamma} = \gamma/(1 + i\Omega\tau). \tag{7e}$$

$$\begin{bmatrix} k - \frac{1}{V_{g1}}\Omega + D(\Omega) + \tilde{\gamma}\left|E_1^0\right|^2 & \tilde{\gamma}\left|E_1^0\right|^2 & 2\tilde{\gamma}E_1^0E_2^0 & 2\tilde{\gamma}E_1^0E_2^0 \\ \tilde{\gamma}|E_1^0|^2 & -k + \frac{1}{V_{g1}} + \tilde{D}(\Omega) + \tilde{\gamma}\left|E_1^0\right|^2 & 2\tilde{\gamma}E_1^0E_2^0 & 2\tilde{\gamma}E_1^0E_2^0 \\ 2\tilde{\gamma}E_1^0E_2^0 & 2\tilde{\gamma}E_1^0E_2^0 & k - \frac{1}{V_{g2}}\Omega + E(\Omega) + \tilde{\gamma}\left|E_2^0\right|^2 & \tilde{\gamma}\left|E_2^0\right|^2 \\ 2\tilde{\gamma}E_1^0E_2^0 & 2\tilde{\gamma}E_1^0E_2^0 & \tilde{\gamma}|E_2^0|^2 & -k + \frac{1}{V_{g2}} + \tilde{E}(\Omega) + \tilde{\gamma}\left|E_2^0\right|^2 \end{bmatrix}. \tag{8}$$

The matrix has nontrivial solution only when the wave number k satisfies the dispersion relation as follows:

$$\left[\left(k - \frac{1}{V_{g1}}\Omega - \frac{1}{6}\beta_{31}\Omega^3\right)^2 - h_1\right] \times \left[\left(k - \frac{1}{V_{g2}}\Omega - \frac{1}{6}\beta_{32}\Omega^3\right)^2 - h_2\right] = C_{\text{XPM}}. \tag{9}$$

The above dispersion relation is the deterministic of the stability of the steady-state solution against the harmonic perturbation. The parameter of the equation can take the form, respectively, as follows:

$$h_j = \left(\tfrac{1}{2}\beta_{2j}\Omega^2 - \tfrac{1}{24}\beta_{4j}\Omega^4\right) \times \left[\tfrac{1}{2}\beta_{2j}\Omega^2 - \tfrac{1}{24}\beta_{4j}\Omega^4 + 2\tilde{\gamma}_j\left|E_j^0\right|^2\right], \tag{10}$$

$$C_{\mathrm{XPM}} = 16\tilde{\gamma}_1\tilde{\gamma}_2\left|E_1^0\right|^2\left|E_2^0\right|^2\left(\tfrac{1}{2}\beta_{21}\Omega^2 - \tfrac{1}{24}\beta_{41}\Omega^4\right)\left(\tfrac{1}{2}\beta_{22}\Omega^2 - \tfrac{1}{24}\beta_{42}\Omega^4\right) \quad (11)$$

The above expression looks similar to the case of dispersion relation corresponding to the case of second-order dispersion (SOD). The difference being the definitions of the parameters h_1, h_2, and C_{XPM} varies from the (SOD) case. Unlike the case of scalar MI, where the odd order dispersion parameters are literally insignificant in the MI dynamics, here in the case of XPM, the odd order dispersion plays a sizable role. For instance, the walk-off effect in the case of SOD consists of only the conventional group velocity mismatch (GVM), whereas, the walk-off effects here constitute both the GVM and also the difference of the third-order dispersion (TOD). Although the TOD difference is not fundamental to the existence of MI, the inclusion of TOD certainly changes the MI dynamics and eventually makes the calculation more complex. For simplicity, we consider the well-known assumption as follows: $\delta_1 = V_{g1}^{-1} - V_{g2}^{-1}$, $\delta_2 = \beta_{31} - \beta_{32}$, and $\mathbf{K} = k - \Omega V_{g2} - (1/6)\beta_{32}\Omega^3$, where δ_1 and δ_2 correspond to the GVM and TOD difference, respectively. After some mathematical manipulations, Eq. (9) can be written in a compact form as

$$\left[\left(\mathbf{K} - \delta_1\Omega - \tfrac{1}{6}\delta_2\Omega^3\right)^2 - h_1\right][\mathbf{K}^2 - h_2] = C_{\mathrm{XPM}}. \quad (12)$$

The distinct MI gain spectra correspond to solutions of the above Eq. (12). For the case of instantaneous nonlinear response ($\tau = 0$), it is straightforward to notice that the dispersion relation is a fourth-order polynomial in **K** with real coefficients leading to four distinct solutions. Out of the four solutions, two are always real and thus insignificant as far as MI is concerned. But the rest of the two are most probably a complex conjugate pair, thereby participating in the MI dynamics and thus ensuring the possibility of only one unstable mode leading to a gain in the band. Now, including the delay in the nonlinear response, it is evident from the dispersion relation [Eqs. (9) and (12)] that any finite value of relaxation time ($\tau \neq 0$), h_j and C_{XPM} become complex thus producing an imaginary part to the wave vector K at any frequency irrespective of the nature of the dispersion regime and thereby extending the frequency range of unstable harmonic perturbation [30]. For any finite value τ, Eq. (12), results in a fourth-order polynomial with complex coefficients. Since the complex roots do not appear in conjugate pairs, this leads to the possibility of two unstable modes for a given frequency Ω [47]. Thus, incorporation of delay in the XPM leads to two unstable modes, in contrast to one in the case of the instantaneous system. The inclusion of HOD, walk-off effect, and delay in the coupled system is extremely difficult to solve, hence a numerical approach is generally preferred.

For the sake of completeness and also to provide a self-explanatory note of the underlying problem, we here intend to recollect some of the much needed results. It is a proven fact that when the wave number K becomes real, obviously the steady-state solution is stable and the harmonic perturbation is purely oscillatory in nature. However, for the case of imaginary K, the steady-state solution is unstable and the perturbation grows exponentially along the length of the fiber, which eventually leads to the breakup of the CW into a train of ultrashort pulses. The corresponding MI gain can be defined as $g(\Omega) = 2\,\mathrm{Im}\{K\}$. K can be calculated numerically from Eq. (12). For instance, we consider the case of scalar MI with the instantaneous nonlinear response ($\tau = 0$), by making either C_{XPM} or one of the h_j in Eq. (12) zero. Now, Eq. (7) reduces the conventional dispersion relation of the scalar-type MI process as follows:

$$\mathbf{K} = \frac{\Omega}{v_{gj}} \pm \sqrt{h_j}. \quad (13)$$

The above case can be addressed in two distinct ways depending upon the propagation wavelength with respect to zero dispersion wavelength, (i) normal dispersion regime, and (ii) anomalous dispersion regime. In the case of normal dispersion regime, there can be two possible cases: (a) $\beta_2 > 0$ and $\beta_4 > 0$, and (b) $\beta_2 > 0$ and $\beta_4 < 0$. For both β_2 and β_4 taking positive values $h_j > 0$; hence $\mathbf{K} \in \mathrm{Re}$, which means that the steady-state solution is stable against the harmonic perturbation and it is purely oscillatory. However, the case $\beta_2 > 0$ and $\beta_4 < 0$ leads to modulation gain even when $\beta_2 > 0$; this is attributed to the fact that the negative value of $\beta_4 < 0$ contributes the required phase matching for the MI process to occur [49,50]. Thus by virtue of the negative value of FOD one can achieve MI even at the normal dispersion regime. The latter case is the anomalous dispersion regime, a familiar case that ensures MI irrespective of the sign of β_4, since any one of the two even order dispersion components or both can contribute to the required phase matching (PMC). Thus for both (c) $\beta_2 < 0$ and $\beta_4 < 0$, and (d) $\beta_2 < 0$ and $\beta_4 > 0$, $\mathbf{K} \in \mathrm{Re}^*$ and hence the harmonic perturbation grows exponential with fiber length. A comprehensive analysis of the scalar MI with HOD under different parametric cases was discussed in Refs. [48–50].

Now, we consider the co-propagation of two optical beams inside fiber with the same polarization; this involves the XPM coupling between the optical field. The XPM with HOD is tricky and requires a good understanding about the role of the individual effects. We consider both the typical cases of the propagation regime: (i) normal dispersion regime and (ii) anomalous dispersion regime. As a matter of fact, the propagation of an individual intense beam in the normal dispersion regime is not subject to MI. Thus in order to achieve MI at least one of the dispersion coefficients needs to take negative values. Interestingly, MI occurs even when both β_2 and β_4 take positive values. This can be made possible only through the XPM effects by means of coupling between the co-propagating beams. In this context, MI occurs solely due to the effect of XPM, thus for any values of the dispersion coefficient the steady-state solution becomes unstable and leads to the exponential growth of the perturbation. Thus the nonlinear coupling between two different modes by XPM extends the domain of MI to the normal GVD regime. It is to be noted that if any of the field vanishes then $C_{\mathrm{XPM}} = 0$ and MI no longer exist. The latter case of the anomalous dispersion regime is relatively easier to understand, since the dispersion coefficients (either both or one) can take negative values and eventually lead to MI. The role of XPM here is to enhance the MI [4,5].

After the detailed introductory ideas about the XPM-MI, we now move on to the objective of the paper. We organized our analysis twofold: (i) effect of walk-off on

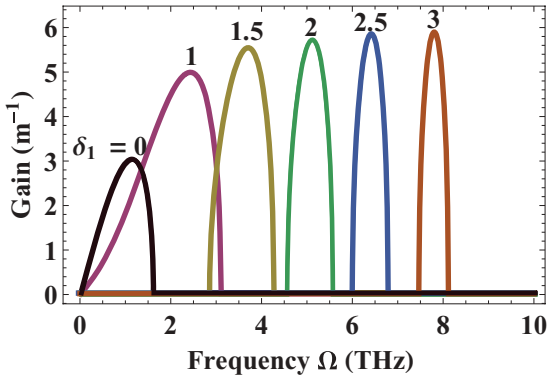

FIG. 1. (Color online) The MI gain spectra $G(\Omega)$ with the effect of GVM for different values of δ_1(ps m^{-1}).

the XPM-MI spectrum, and (ii) impact of finite relaxation time in the MI spectrum. In order to give a comprehensive picture of the role of walk-off and HOD in the MI spectrum, we consider both normal and anomalous dispersion regimes. Without loss of generality, we consider the dispersion parameters as $\beta_2 = \beta_{21} = \beta_{22} = \pm 60$ ps^{2}km^{-1}, $\beta_4 = \beta_{41} = \beta_{42} = 0.1$ ps^{4}km^{-1} and the nonlinear parameter $\gamma_1 = \gamma_2 = 15\,\mathrm{W}^{-1}\mathrm{km}^{-1}$. The input optical powers are set as $P_1 = 100$ W and $P_2 = 100$ W. The TOD difference can vary in the range $\delta_2 = 0 - 6 \times 10^{-4}\mathrm{ps}^3 m^{-1}$ and the group velocity mismatch varies in the range $\delta_1 = 0$–4 ps m^{-1}.

IV. EFFECT OF WALK-OFF ON XPM IN THE NORMAL DISPERSION REGIME

The scenario in which both beams experience a normal GVD is of particular importance since MI may occur solely by virtue of the XPM. Thus in the present section we intend to provide a detailed analysis of the interplay between walk-off and HOD. In order to make the discussion clear, subsections are made to study the impact of various physical effects in detail.

A. In the case of $\delta_1 \neq 0$ and $\delta_2 = 0$

To illustrate the role of HOD and the walk-off effect in the MI spectrum, first the interplay between FOD and GVM (δ_1) is analyzed. For the case ($\delta_1 \neq 0$ and $\beta_4 = 0$), it is observed

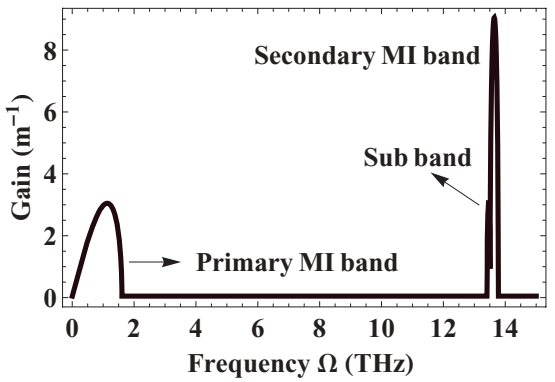

FIG. 2. The MI gain spectra $G(\Omega)$ with the effect of FOD in the absence of GVM.

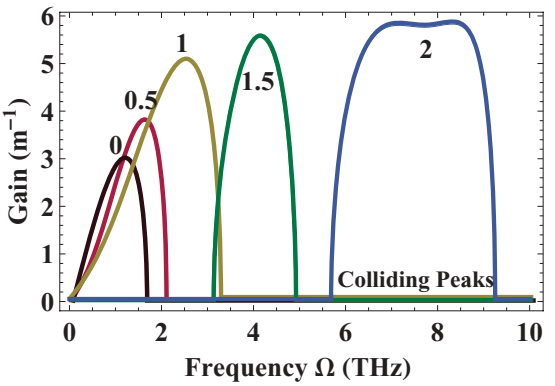

FIG. 3. (Color online) First MI spectral window with the effect of FOD and GVM for various values of δ_1.

from Fig. 1, as δ_1 increases the instability band shifts towards the higher frequencies and the corresponding bandwidth decreases considerably with its peak approaching a limiting value. Whereas inclusion of β_4 dramatically changes the MI spectrum, where new spectral bands evolve at characteristic frequencies given by the dispersion relation. It is apparent from Fig. 2, for the null group velocity mismatch the MI spectrum consists of two distinct bands, one at near- and the other at far-from-center frequencies. It is to be noted that the second spectral band consists of a subordinate spectral band with reduced gain. For better understanding about the influence of GVM and FOD on the MI spectrum, the spectral window has been divided into two segments. Incorporation of GVM qualitatively changes the MI spectrum, like shape, position, and the number of spectral peaks. The evolution of a new spectral band is obvious from Figs. 3 and 4. Incorporation of GVM brings in new characteristic spectral spikes at different frequencies as given by the dispersion relation Eq. (12).

For a particular case ($\delta \neq 0$ and $\beta_4 \neq 0$), the second spectral window is interesting and consists of an immobile primary central band with two mobile secondary spectral spikes on either side of the central band. With increase in the value of the GVM, the central band remains stationary whereas the secondary spectral spikes moves away from the central band. On the contrary, the increase in the GVM shifts the first spectral band towards higher frequencies; for a particular value of GVM the first spectral band collides with one of the

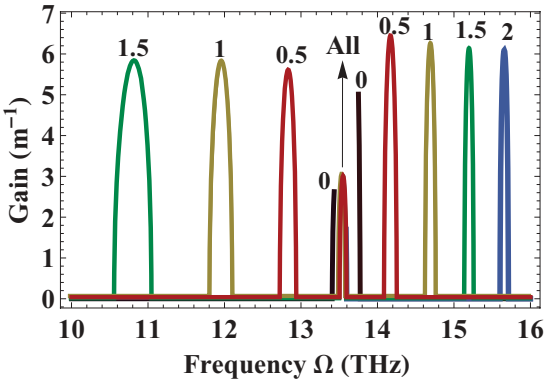

FIG. 4. (Color online) Second spectral window of MI with the combined effect of GVM and FOD.

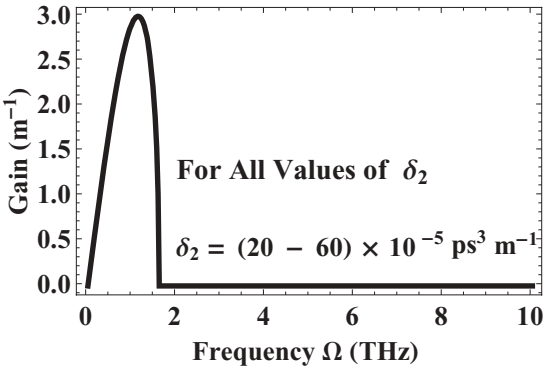

FIG. 5. The first MI spectral window of null GVM for different values of δ_2 with the effect of β_4.

secondary spectral spikes moving towards the center frequency as shown in Fig. 3.

B. In the case of $\delta_1 = 0$ and $\delta_2 \neq 0$

We now shift our attention to analyze the walk-off effect by virtue of TOD. For instance, we consider $\delta_1 = 0$ and $\delta_2 \neq 0$ to study exclusively the influence of TOD on the MI spectrum.

The influence of HOD effects like TOD and FOD are interesting and lead to a rich variety of information about the MI dynamics in most practical scenarios. Quite clearly, the role of TOD is similar to the case of the GVM.

Figures 5 and 6 show the gain spectrum of MI for different values of δ_2. As in the previous section, the MI spectrum consists of two distinct spectral windows. Like the earlier case, with an increase in δ_2 the first spectral band remains stationary and the two secondary spectral spikes on either side of the immobile primary central band in the second spectral window move away from the primary central band.

C. In the case of δ_1 and $\delta_2 \neq 0$

Here, we will discuss the interplay between the walk-off effect and HOD under the combined action of GVM and TOD. In order to analyze the above, we consider the case of $\delta_1 \neq 0$ and $\delta_2 \neq 0$.

Figures 7 and 8 depict the MI spectrum for some representative cases of δ_1 and δ_2. It is observed that like in the previous

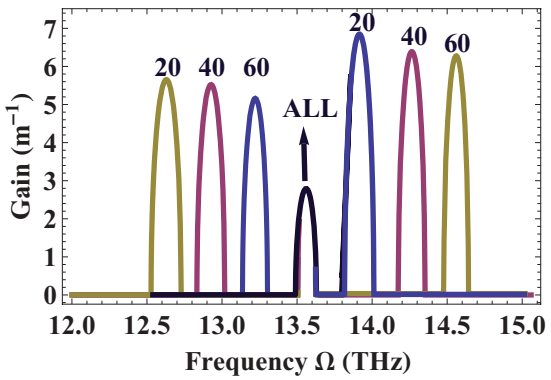

FIG. 6. (Color online) The second spectral window for the combined effect of δ_2 and β_4 for null GVM.

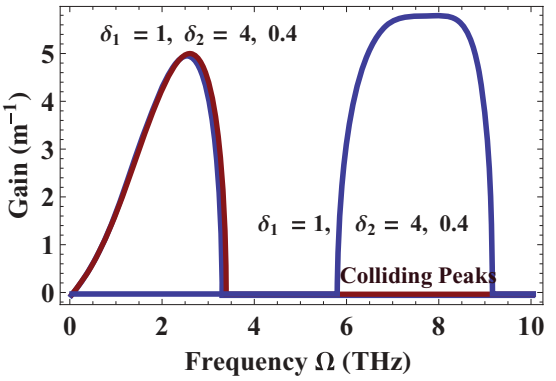

FIG. 7. (Color online) First MI spectral window for the combined effect of FOD and walk-off (both the GVM and TOD difference) for different combinations of δ_1 and δ_2.

cases of varying δ_1 and δ_2, here, too, many of the results coincide. Thus, one can conclude that the increase in either δ_1 or δ_2, or both, leads to the shift of the first spectral band to the higher frequency side and the two secondary spectral spikes on either side of the primary central band moves apart. For a particular value of either δ_1 or δ_2, the first spectral band collides with one of the secondary spectral spikes and evolves as a single band.

Figures 1–8 portray the evolution of a new spectral band due to the HOD effects. It is obvious from these figures that the instability region is no longer continuous as in the case of the GVD dominant system; rather it is discrete with localized MI gain peaks. We observed from our calculation, when $\tau \to 0$, the system switch back to the conventional Kerr-type nonlinear case ($\tilde{\gamma} \to \gamma$) and our Eq. (12) coincides completely with Eq. (11) of Ref. [53]. Moreover, one can infer from Figs. 1–8 that our findings agree readily with Ref. [53], except for the change in the numerical value of quantities such as G (Ω) and Ω; this is obvious because of the different values of the variables handled in the context. Unlike the case ($\delta \neq 0$ and $\beta_4 = 0$), where there exists one critical GVM (δ_c) above which the MI gain occurs at a finite frequency range, for $\beta_4 \neq 0$, in addition to the instability band near center frequency, there exist three more distinct spectral bands on the longer frequency side, each corresponding to a characteristic frequency width

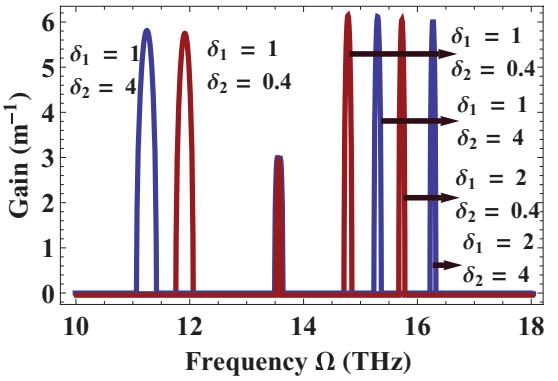

FIG. 8. (Color online) Second spectral window of MI for different combinations of δ_1(ps m^{-1}) and δ_2(10^{-4} ps^3 m^{-1}) with the effect of FOD.

determined by the parameters of the dispersion relation. Thus the critical GVM as stated in Ref. [47], has to be redefined with the required modification. In the case of ($\delta \neq 0$ and $\beta_4 \neq 0$), the δ_c required for the evolution of MI with finite bandwidth can only be applicable to the first spectral band and can take the value $\delta_c = 1.0395$, whereas the second spectral window emerges inevitably for all δ_1. The above agreement fairly holds for the δ_2 with the parameter values being different. Thus this section concludes that incorporation of δ_1 and δ_2 leads to a threshold behavior for the evolution of the MI band at finite frequency. But the evolution of the spectral band in the secondary spectral window occurs spontaneously for all finite values of δ_1 and δ_2. Thus the incorporation of HOD and walk-off effect in the XPM leads to four discrete instability regions (one near the center frequency and three far from center frequency). Therefore the unstable region of MI can be written in a simplified notation as $\Omega_i^{\min} < \Omega < \Omega_i^{\max}$, where i at 1, 2, 3, and 4 corresponds to the unstable MI bands (numbering is from the center to the extreme band).

V. EFFECT OF WALK-OFF EFFECT ON XPM IN THE ANOMALOUS DISPERSION REGIME

This section deals with the practicable case of pulse propagation, where β_2 takes negative values and thereby produces MI without the aid of the XPM. Although XPM has nothing to do with the origin of the MI band, it plays a crucial role in the characteristics of the MI band, thus making the study of walk-off effect on XPM in the anomalous GVD necessary. We proceed along similar lines as discussed earlier by dividing into subsections, so as to appreciate the importance of individual effects on MI spectrum.

A. In the case of $\delta_1 \neq 0$ and $\delta_2 = 0$

In this case walk-off effect consists of only the conventional GVM, and the TOD difference is temporarily disabled by making $\delta_2 = 0$. For the anomalous GVD regime, β_2 possesses negative value, and FOD as in the previous case is maintained as $\beta_4 = 0.1\ \mathrm{ps}^4\,\mathrm{km}^{-1}$ throughout our discussion. It is worth noting from Fig. 9 that the inclusion of β_4 hardly has any effect on the MI spectrum, since there exists only one MI band. This is in contrast to the case of normal GVD, where two MI bands, one at near- and the other at far-from-center frequency is observed. This absence of the secondary band in the higher frequency side is attributed to the opposite sign of β_2 and β_4. The two dispersion effects compete with each other due to the opposite nature of their signs, and, for the parameters chosen in our case, it is quite evident that β_2 dominates and leads to the characteristic MI band near the center frequency by eliminating the FOD bands on the far-frequency side.

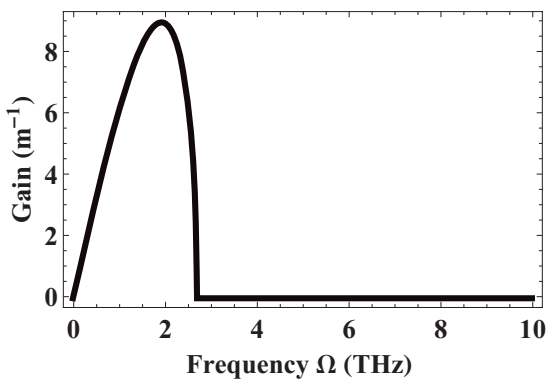

FIG. 9. The MI gain spectra $G(\Omega)$ with the effect of FOD in the absence of GVM.

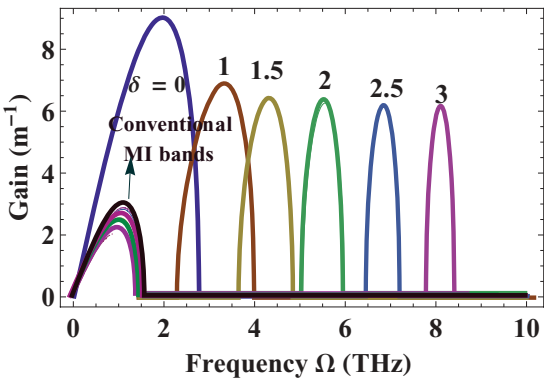

FIG. 10. (Color online) The MI gain spectra $G(\Omega)$ with the effect of GVM for different values of $\delta_1(\mathrm{ps\,m}^{-1})$.

Now we turn our attention towards the walk-off effect ($\beta_2 = -60\,\mathrm{ps}^2\,\mathrm{km}^{-1}$, $\beta_4 = 0$); it is to be noted that with increase in the δ_1, the MI band as usual shifts towards the higher frequency side, but the peak gain matters here. In the earlier case of normal GVD, with increase in GVM the MI band shifts towards the higher frequency side and the peak gain increases gradually until it saturates after a certain finite value of δ_1. However, in the anomalous GVD case, the behavior of the peak gain is the opposite (i.e., peak gain decreases from the maximum and saturates after a certain value of δ_1) as is evident from Fig. 10. Now, we consider the combination of ($\beta_4 \neq 0, \delta_1 \neq 0$) as in Fig. 11; here unlike the normal GVD case there is no secondary spectral window at the higher frequency region, which is a consequence of the weak contribution by FOD. Moreover, in addition to the finite frequency band due to GVM, one can also observe the conventional MI band owing to the dominance of SOD over other effects. The effect of walk-off (only δ_1) as expected shifts the MI band towards the higher frequency side with an increase in the GVM.

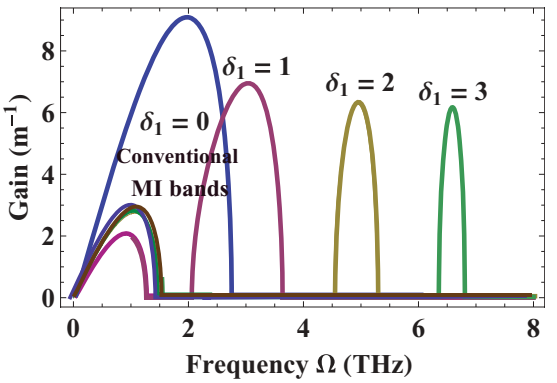

FIG. 11. (Color online) The MI spectra $G(\Omega)$ with the effect of FOD and GVM for various values of δ_1.

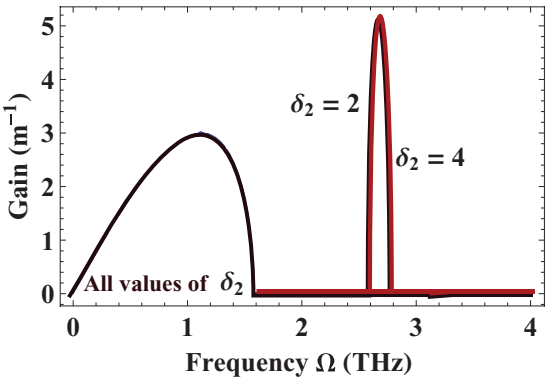

FIG. 12. (Color online) The MI spectra for the combined effect of $\delta_2(10^{-4}$ ps^3 m$^{-1})$ and β_4 for null GVM.

B. In the case of $\delta_1 = 0$ and $\delta_2 \neq 0$

Now consider the walk-off effect due to the TOD difference. Two distinct bands can be observed from Fig. 12: One near the center frequency is the characteristic of the anomalous GVD and the other away from the center corresponds to the walk-off effect caused solely by the TOD difference.

It is evident from Fig. 12, like the case of GVM, increasing δ_2 shifts the MI band towards the longer wavelength side, but very slightly. There is no evidence of secondary spectral bands in the higher frequency side here, which is the signature of the weak contribution by β_4 and the relative dominance of the GVD effect.

C. In the case of δ_1 and $\delta_2 \neq 0$

Here, we consider the interplay between HOD and walk-off under the combined actions of δ_1 and δ_2. Two distinct spectral bands can be observed at near- and far-from-center frequency. To illustrate some representative combination of β_4, δ_1 and δ_2 are considered. It is obvious from Fig. 13 that the TOD difference is indeed very weak, and the major contribution to walk-off effect comes considerably from the GVM effect. As discussed earlier, the walk-off, as usual, shifts the spectral band towards higher frequency. Increase in the δ_1 actually determines the shift of the finite frequency band and δ_2 is found to be relatively weak. In addition, the increase in δ_1 brings a modest decrease in the peak gain of the conventional MI band near the center frequency, which is apparent from Fig. 13.

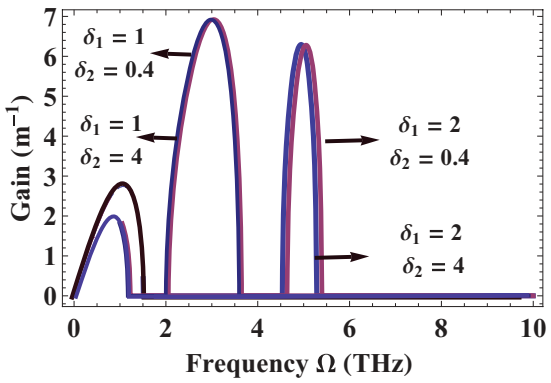

FIG. 13. (Color online) The MI spectra with the effect of FOD and the walk-off for different combinations of δ_1(ps m^{-1}) and $\delta_2(10^{-4}$ ps^3 m$^{-1})$.

It is noteworthy that the inclusion of walk-off effect, as usual, results in the discrete instability band. Unlike the existence of four unstable bands for the normal dispersion regime, here in the case of the anomalous GVD regime only two discrete bands are observed. The critical unstable frequency can be written as $\Omega_i^{\min} < \Omega < \Omega_i^{\max}$, where i can take 1, 2 corresponding to two unstable MI bands.

VI. ROLE OF RELAXATION OF NONLINEAR RESPONSE IN THE NORMAL DISPERSION REGIME OF THE MI SPECTRUM

It is worth noting from our mathematical treatment of linear stability analysis, any finite relaxation time (τ) in the nonlinear response leads to the imaginary part of K for any frequency. Thus, this leads to the evolution of two MI curves as a consequence of two unstable modes for a given frequency. The unstable modes are recognized as Raman modes due to the retarded nature of the nonlinear responses. In order to figure the role of HOD, GVM, and delay on MI, we have divided this section into subsections to exclusively explore the individual effects on the MI spectrum.

A. In the case of β_4, $\tau \neq 0$ and $\delta = 0$

In this case, the walk-off effect is made zero ($\delta = 0$), in order to analyze the effect of HOD and delay (τ) on MI. Here, the parameter δ stands for the total walk-off contribution due to both GVM and the TOD difference ($\delta = \delta_1 + \delta_2$). The inclusion of FOD leads to the evolution of the secondary sidebands at a characteristic frequency. In Fig. 14 two spectral regions corresponding to the two MI bands are observed: The former is close to the pump frequency and the latter is the FOD band. For the case of short or fast response (small value of τ), the first MI band (instantaneous band) remains unaffected, whereas the second MI band suffers a decrease in the gain with the inclusion of delay, which is apparent from Fig. 14. The role of delay is interesting, since any finite value of τ extends the range of unstable frequencies, for instance, due to the small

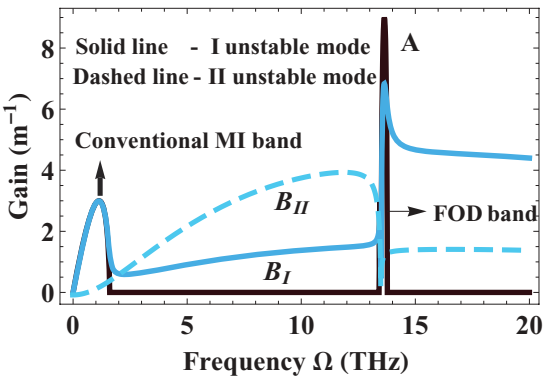

FIG. 14. (Color online) The MI gain spectra without walk-off effect for the case of instantaneous ($\tau = 0$) and delayed nonlinear response with FOD. The nonlinear response is said to be a fast response ($\tau = 0.01$ ps).

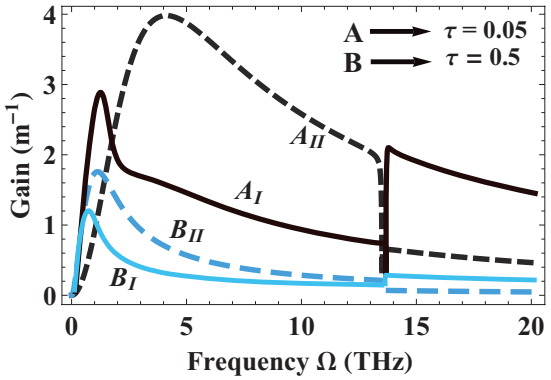

FIG. 15. (Color online) The MI gain spectra for the case of slow response in the presence of FOD and the absence of walk-off.

value of τ the instability region extends all the way from the primary sideband to the secondary band and eventually connects the two MI bands. The second mode, which becomes unstable due to the delayed nonlinear response (dashed curve), shows a larger average MI gain than the primary band of the first unstable mode but the dominance of FOD sets a fall in the MI gain and the retarded Raman response extends the unstable frequency range.

Now, for the case of slow response (large value of τ) the dynamics evolve differently. Although, in principle, the delay results in the infinite unstable frequency, the slow response generally leads to the overall suppression of MI. We consider some representative cases of delay time in Fig. 15; it can be observed that for larger value of τ the MI gain suffers and registers the least gain factor for slow responses. No distinct FOD peak is observed as in the fast response case, which infers that delay suppresses even the dominant FOD effects. Moreover, the second unstable mode (represented by the dashed curve) records a larger gain factor than the first mode; a sudden fall at the higher detuning frequency is observed, which is a manifestation of the counteraction of the slow response over the FOD peak.

B. In the case of β_4, $\tau \neq 0$ and δ_1 and $\delta_2 \neq 0$

The inclusion of walk-off effects dramatically changes the MI spectrum and leads to the emergence of a new spectral band

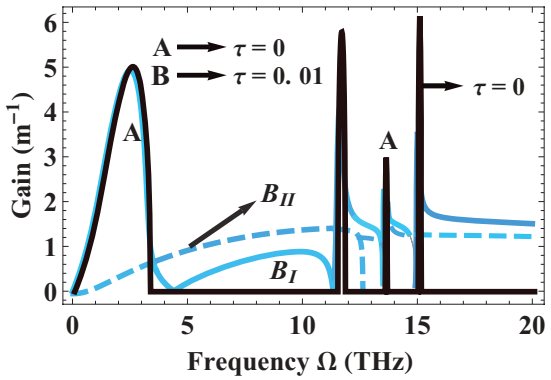

FIG. 16. (Color online) The MI gain spectra under the combined action of FOD and walk-off effect ($\delta_1 = 1\,\mathrm{ps\,m^{-1}}$ and $\delta_2 = 4 \times 10^{-4}\,\mathrm{ps^3\,m^{-1}}$) in the regime of fast and instantaneous response.

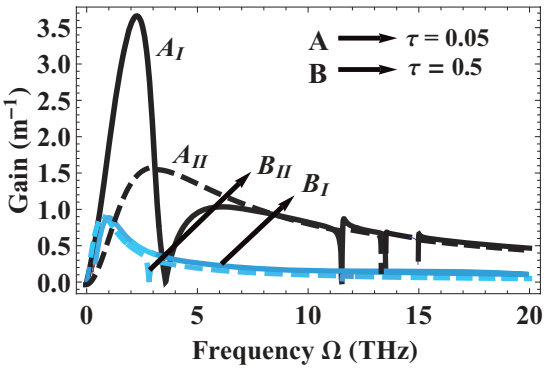

FIG. 17. (Color online) The MI gain spectra under the combined action of FOD and walk-off effect in the regime of slow responses.

with finite frequency width as observed in the previous section. The walk-off effect here constitutes the combined effects of GVM (δ_1) and the TOD difference (δ_2). It is noteworthy that each band corresponds to a finite frequency width and thus the unstable frequency window is discrete. However, the incorporation of delay extends the unstable frequency window by connecting the individual localized unstable bands. Thus, unlike the instantaneous case, where the unstable regions are discrete, here in the case of the delayed system the unstable window is continuous and runs all the way from the pump frequency literally down to an infinite frequency range. For the case of fast response, one can readily observe from Fig. 16 that the instantaneous band remains unaffected, whereas the delay qualitatively suppresses the gain of the other MI bands. The second unstable mode (dashed curve) possesses lesser gain factor and a hump corresponding to the FOD peak (MI band due to FOD) thus ensures the relative dominance of the FOD effect.

Now we consider the slow response time, as predicted earlier; here, too, slow response suppresses the MI. Two representative cases of delay time are considered as shown in Fig. 17; it is observed that the larger delay time leads to significant decreases in the MI gain of the primary band (near center frequency). It can also be noted that the increase in the delay time (slow response) considerably decreases the gain factor of the other MI band originates due to walk-off and FOD. The behavior of the second spectral mode is the same as the fast response (i.e., reduced gain factor with a hump at the FOD peak).

VII. ROLE OF RELAXATION OF NONLINEAR RESPONSE IN THE ANOMALOUS DISPERSION REGIME OF THE MI SPECTRUM

A. In the case of β_4, $\tau \neq 0$ and $\delta = 0$

Here, the co-propagation of two beams in the anomalous dispersion regime is considered, where β_2 takes negative value, thereby supporting MI without the aid of the XPM. In this context, the role of XPM is to support MI and enhance its effect in parallel with the GVD effects.

Our analysis of the impact of delay in the nonlinear response over the MI spectrum follows in a similar way as the proceeding section. First, we consider the null GVM effect, in order to analyze the impact of HOD and delay on

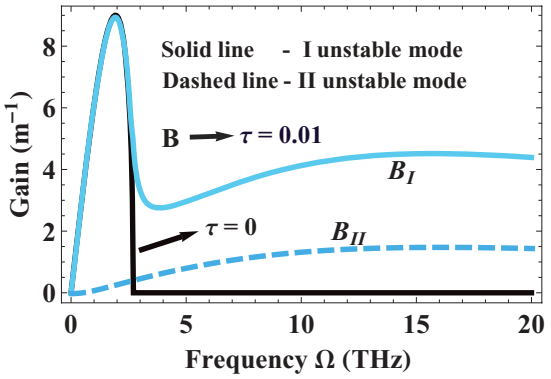

FIG. 18. (Color online) The MI gain spectra without walk-off effect for the case of instantaneous ($\tau = 0$) and fast response ($\tau = 0.01$ ps) with the effect of FOD.

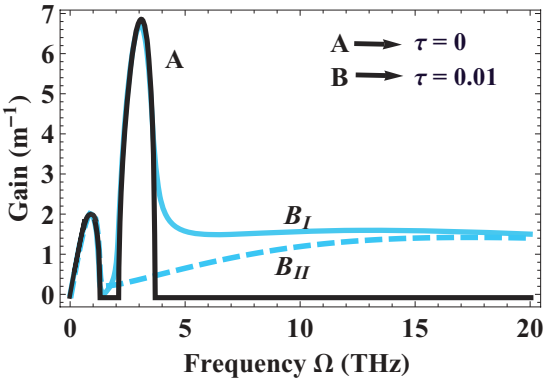

FIG. 20. (Color online) The MI gain spectra under the combined action of FOD and walk-off effect ($\delta_1 = 1$ ps m^{-1} and $\delta_2 = 4 \times 10^{-4}$ ps^3 m^{-1}) in the regime of fast and instantaneous response.

MI. The inclusion of FOD hardly brings any changes to the MI spectrum; this is mainly due to the relative dominance of anomalous GVD over FOD. For the parameters $\beta_2 = -60$ ps^2 km^{-1} and $\beta_4 = 0.1$ ps^4 km^{-1}, β_2 dominates over β_4 and masks the characteristics of FOD. Therefore, there exists only one MI band corresponding to the conventional anomalous GVD effects.

Now consider the role of delay in the nonlinear response (we initially consider the fast response); it is evident from Fig. 18 the delay extends the range of unstable frequencies and induces two MI curves corresponding to two unstable modes. The first mode of unstable frequency consists of a primary band of the same gain as that of the instantaneous band, which further extends to the higher frequencies. The second mode due to the delayed nonlinear response consists of unstable frequency of reduced gain. Figure 19 portrays MI spectrum for some representative case of slow responses. It is obvious from our earlier argument, and here, too, the increase in the delay time leads to decrease in the gain, thereby suppressing the overall MI.

B. In the case of β_4, $\tau \neq 0$ and δ_1 and $\delta_2 \neq 0$

Now we include the walk-off effect in the picture, by considering GVM (δ_1) and the TOD difference (δ_2) of the co-propagating beams. A particular combination of δ_1 and δ_2 is considered. Due to the walk-off effect new spectral bands originate, one near the center frequency and the other far from the center frequency. No other spectral bands occur as in the normal GVD case, which is purely due to the weaker contribution of FOD. Incorporation of delay connects the two spectral bands and further extends the range of unstable frequencies. For the case of fast response, it is apparent from Fig. 20 that the delay hardly disturbs the gain of the MI bands but extends the instability window to longer frequency range.

Figure 21 illustrates the role of slow response, as well established in the earlier section; here, also, slow response inevitably suppresses the MI by reducing the gain factor. It is pretty clear from Fig. 21 that increases in the delay time certainly decrease the MI gain of both the unstable modes.

VIII. SUMMARY AND CONCLUSION

In summary, we have investigated the XPM-induced MI in the system of relaxing Kerr nonlinearity under the influence of HOD and walk-off effect. Using the Debye relaxational model, a time-dependent nonlinear response is incorporated in the system of CNLSE to account for the delay in the nonlinear response. The governing dynamical equation is suitably modeled to include the cumulative effect of HOD and walk-off [Eq. (1)]. First, we analyzed the role of HOD and walk-off effect in the XPM-induced MI for both the dispersion regimes. In the normal GVD regime, the HOD

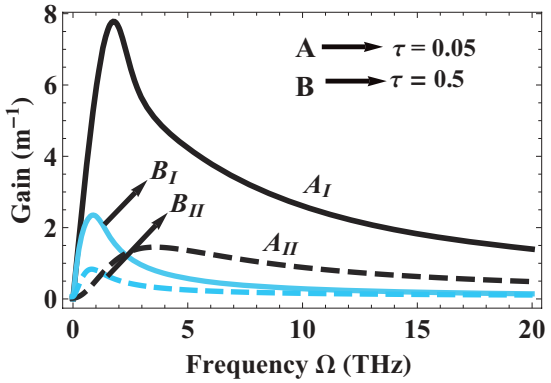

FIG. 19. (Color online) The MI gain spectra for the case of slow responses with the effect of FOD and the absence of walk-off.

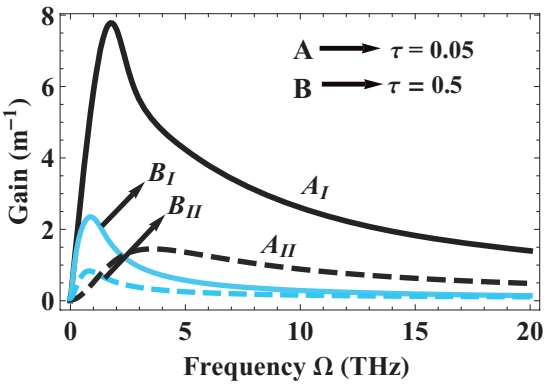

FIG. 21. (Color online) The MI gain spectra under the combined action of FOD and walk-off effect in the regime slow responses.

and walk-off effect brings new characteristic spectral bands at a definite frequency window. The walk-off effect consists of both the GVM and the TOD difference and it is observed that both play identical roles in the MI dynamics. In general, increase in the walk-off (δ) shifts the MI band towards the higher frequency side and also leads to new spectral bands. Four discrete spectral bands are observed, which have been divided into two spectral windows. The first spectral window consists of a single band near the center frequency and the spectral window consists of three bands: one immobile primary band and two mobile secondary bands on either side of the primary band, respectively (Figs. 1–8). Increase in (δ) shifts the mobile band away from the primary center band. In the anomalous GVD regime (Figs. 9–13), there exist two bands, one near and the other away from the center frequency. This is attributed to the fact that for the anomalous GVD regime, FOD is relatively suppressed due to the dominance of SOD. There is no observation of a secondary spectral band and the role of walk-off effect is found to be the same as that of the normal GVD case.

Later, we discussed exclusively the influence of relaxation in the nonlinear response for both dispersion regimes. The role of delay is addressed in two typical cases, namely (a) fast response and (b) slow response. The cumulative effect of HOD, walk-off, and the delay leads to interesting behavior as follows: (i) Any finite relaxation extends the range of unstable frequencies and there exist two unstable modes called the Raman mode; (ii) in the normal GVD regime (Figs. 14–17), there exist four discrete unstable MI bands for the case of instantaneous response. Inclusion of delay (τ) makes the MI curve run through the local instability bands and thereby extends the range of unstable frequencies literally down to infinite frequency. (a) For the case of fast response, the incorporation of delay hardly has any impact on the first band, whereas the rest of the MI bands undergo a relative fall in the gain. The second unstable mode possesses the larger gain factor and a hump corresponding to the FOD band. (b) The slow response reduces the MI gain thereby suppressing the overall MI. (iii) In the case of the anomalous GVD regime (Figs. 18–21), there exist two discrete MI bands. The delay as discussed earlier extends the unstable frequencies and connects the two MI bands. (a) For the fast response, the gain of the first band remains unaffected, whereas the second band suffers a slight fall in the gain. (b) The slow response, however, extends the unstable frequencies but suffers MI by depleting the overall MI gain. Overall, the relaxation in the nonlinear response offers infinite unstable frequencies. The walk-off effect and HOD, on the other hand, bring a new characteristic local MI band. Thus the combined action of both walk-off and HOD effects are responsible for the generation of the MI spectrum, where the MI curve looks like it is sailing over the local instability bands. To wrap up, the combination of HOD and the relaxation effect in coupled system leads to a rich variety of information, which requires experimental realization. We believe that the outcome of the article can set the benchmark for experiments pertaining to the investigation of various nonlinear effects in the relaxing nonlinear system.

ACKNOWLEDGMENTS

K.P. thanks Department of Science and Technology (DST), Department of Atomic Energy-Board of Research in Nuclear Sciences (DAE-BRNS), and University Grants Commission (UGC), Government of India, for financial support through major projects.

[1] G. Agrawal, *Nonlinear Fiber Optics*, 4th ed. (Academic Press, San Diego, 2007).
[2] G. Agrawal, *Application of Nonlinear Fiber Optics*, 2nd ed. (Academic Press, New York, 2001).
[3] A. Ghatak and K. Thyagarajan, *An Introduction to Fiber Optics* (Cambridge University Press, New York, 2000).
[4] G. P. Agrawal, Phys. Rev. Lett. **59**, 880 (1987).
[5] G. P. Agrawal, P. L. Baldeck, and R. R. Alfano, Phys. Rev. A **39**, 3406 (1989).
[6] M. Yu, C. J. McKinstrie, and G. P. Agrawal, Phys. Rev. E **48**, 2178 (1993).
[7] A. Hasegawa and F. Tappert, Appl. Phys. Lett. **23**, 142 (1973).
[8] A. Hasegawa, Opt. Lett. **9**, 288 (1984).
[9] K. Tai, A. Hasegawa, and A. Tomita, Phys. Rev. Lett. **56**, 135 (1986).
[10] S. K. Turitsyn, A. M. Rubenchik, and M. P. Fedoruk, Opt. Lett. **35**, 2684 (2010).
[11] A. M. Rubenchik, S. K. Turitsyn, and M. P. Fedoruk, Opt. Express **18**, 1380 (2010).
[12] J. M. Dudley, G. Genty, and S. Coen, Rev. Mod. Phys. **78**, 1135 (2006).
[13] R. V. Raja., K. Porsezian, and K. Nithyanandan, Phys. Rev. A **82**, 013825 (2010).
[14] K. Hammani, B. Wetzel, B. Kibler, J. Fatome, C. Finot, G. Millot, N. Akhmediev, and J. M. Dudley, Opt. Lett. **36**, 2140 (2011).
[15] M. N. Z. Abouou, P. T. Dinda, C. M. Ngabireng, B. Kibler, and F. Smektala, J. Opt. Soc. Am. B **28**, 1518 (2011).
[16] A. Kumar, A. Labruyere, and P. T. Dinda, Opt. Commun. **219**, 221 (2003).
[17] S. Trillo, S. Wabnitz, G. I. Stegeman, and E. M. Wright, J. Opt. Soc. Am. B **6**, 889 (1989).
[18] T. Sylvestre, S. Coen, P. Emplit, and M. Haelterman, Opt. Lett. **27**, 482 (2002).
[19] S. Coen and M. Haelterman, Opt. Lett. **26**, 39 (2001).
[20] R. Ganapathy, K. Senthilnathan, and K. Porsezian, J. Opt. B **6**, S436 (2004).
[21] M. J. Potasek, Opt. Lett. **12**, 921 (1987).
[22] X. Liu, J. W. Haus, and S. Shahriar, Opt. Commun. **281**, 2907 (2008).
[23] W.-H. Chu, C.-C. Jeng, C.-H. Chen, Y.-H. Liu, and M.-F. Shih, Opt. Lett. **30**, 1846 (2005).
[24] L. Zhang, S. Wen, X. Fu, J. Deng, J. Zhang, and D. Fan, Opt. Commun. **283**, 2251 (2010).
[25] C. Cambournac, H. Maillotte, E. Lantz, J. M. Dudley, and M. Chauvet, J. Opt. Soc. Am. B **19**, 574 (2002).

[26] M.-F. Shih, C.-C. Jeng, F.-W. Sheu, and C.-Y. Lin, Phys. Rev. Lett. **88**, 133902 (2002).
[27] H. Leblond and C. Cambournac, J. Opt. A: Pure Appl. Opt. **6**, 461 (2004).
[28] I. Velchev, R. Pattnaik, and J. Toulouse, Phys. Rev. Lett. **91**, 093905 (2003).
[29] W. Shuang-Chun, S. Wen-Hua, Z. Hua, F. Xi-Quan, Q. Lie-Jia, and F. Dian-Yuan, Chin. Phys. Lett. **20**, 852 (2003).
[30] G. L. da Silva, I. Gleria, M. L. Lyra, and A. S. B. Sombra, J. Opt. Soc. Am. B **26**, 183 (2009).
[31] J. E. Rothenberg, Phys. Rev. A **42**, 682 (1990).
[32] T. Tanemura and K. Kikuchi, J. Opt. Soc. Am. B **20**, 2502 (2003).
[33] P. D. Drummond, T. A. B. Kennedy, J. M. Dudley, R. Leonhardt, and J. D. Harvey, Opt. Commun. **78**, 137 (1990).
[34] G. Millot, E. Seve, and S. Wabnitz, Phys. Rev. Lett. **79**, 661 (1997).
[35] G. Millot, E. Seve, S. Wabnitz, and J. M. Haelterman, J. Opt. Soc. Am. B **15**, 1266 (1998).
[36] S. Trillo and S. Wabnitz, J. Opt. Soc. Am. B **6**, 238 (1989).
[37] E. Seve, G. Millot, S. Wabnitz, T. Sylvestre, and H. Mail-lotte, J. Opt. Soc. Am. B **16**, 1642 (1999).
[38] A. S. Gouveia-Neto, M. E. Faldon, A. S. B. Sombra, P. G. J. Wigley, and J. R. Taylor, Opt. Lett. **13**, 901 (1988).
[39] K. Senthilnathan and K. Porsezian, Phys. Lett. A **301**, 433 (2002).
[40] E. Seve, P. Tchofo Dinda, G. Millot, M. Remoissenet, J. M. Bilbault, and M. Haelterman, Phys. Rev. A **54**, 3519 (1996).
[41] P. T. Dinda, G. Millot, E. Seve, and M. Haelterman, Opt. Lett. **21**, 1640 (1996).
[42] P. T. Dinda, G. Millot, and P. Louis, J. Opt. Soc. Am. B **17**, 1730 (2000).
[43] S. Kumar, A. Selvarajan, and G. Anand, Opt. Commun. **102**, 329 (1993).
[44] P. T. Dinda, S. Wabnitz, E. Coquet, T. Sylvestre, H. Maillotte, and E. Lantz, J. Opt. Soc. Am. B **16**, 757 (1999).
[45] P. T. Dinda and K. Porsezian, J. Opt. Soc. Am. B **27**, 1143 (2010).
[46] Y. Silberberg and I. Bar-Joseph, J. Opt. Soc. Am. B **1**, 662 (1984).
[47] A. A. Canabarro, B. Santos, I. Gleria, M. L. Lyra, and A. S. B. Sombra, J. Opt. Soc. Am. B **27**, 1878 (2010).
[48] F. Abdullaev, S. Darmanyan, S. Bischoff, P. Christiansen, and M. Srensen, Opt. Commun. **108**, 60 (1994).
[49] S. B. Cavalcanti, J. C. Cressoni, H. R. da Cruz, and A. S. Gouveia-Neto, Phys. Rev. A **43**, 6162 (1991).
[50] S. Pitois and G. Millot, Opt. Commun. **226**, 415 (2003).
[51] P. T. Dinda, C. Ngabireng, K. Porsezian, and B. Kalithasan, Opt. Commun. **266**, 142 (2006).
[52] G. Millot, P. Dinda, E. Seve, and S. Wabnitz, Optical Fiber Technology **7**, 170 (2001).
[53] Z. Xian-Qiong and X. An-Ping, Chin. Phys. **16**, 1683 (2007).